ce/papers Proceedings in civil engineering

Ernst & Sohn A Wiley Brand

ORIGINAL ARTICLE

eurosteel AMSTERDAM 2023

Ernst & Sohn A Wiley Brand

Heat management and tensile strength of 3 mm mixed and matched connections of butt joints of S355J2+N, S460MC and S700MC

Stefan Eichler[1] | Mareike von Arnim[2] | Oliver Brätz[3] | Jörg Hildebrand[1] | Andreas Gericke[3] | Jean Pierre Bergmann[1] | Ulrike Kuhlmann[2] | Knuth-Michael Henkel[3]

Correspondence

Stefan Eichler
Technische Universität Ilmenau, Department of Mechanical Engineering, Production Technology Group
Gustav-Kirchhoff-Platz 2
98693 Ilmenau
Email: stefan.eichler@tu-ilmenau.de

[1] TU-Ilmenau, Ilmenau, Germany
[2] University of Stuttgart, Institute of Structural Design, Stuttgart, Germany
[3] Fraunhofer IGP, Rostock, Germany

Abstract

High-strength structural steels are beneficial in terms of the sustainability of constructions due to the possible reduction of weight and overall material needs. Nevertheless, high-strength steels have a smaller processing parameter range in regarding the specific heat input and resulting cooling rate. Especially the cooling time $t_{8/5}$ characterizing the time span to cool down from 800 to 500 °C is an important indicator. Single layer butt-welded gas metal arc welding (GMAW) connections of 3 mm plates between normal strength (S355J2+N, S460MC) and high-strength steels (S700MC) as well as matched connections (S460MC, S700MC) are carried out. Hereby, the influence of the energy input, melting rate, joint preparation, filler metal (matching and undermatching) and backing methods are observed. Spatially resolved IR-thermal observation shows variations within the welds of up to 50 % in the cooling time $t_{8/5}$ depending on those parameters. These fluctuations lead to significant changes of the microstructure within the melting and heat-affected zone. UCI hardness mappings show the softening and microstructural change within these zones. Those soft zones can be the region of failure for butt welded connections as shown by transverse tensile tests with spatially resolved optical strain measurements. The results obtained can be used to define more precise welding procedures of these types of connections and also are used to develop design rules for mixed connections made of normal strength and high-strength steel.

Keywords

mixed connections, butt weld, high-strength steel, tensile test, heat-affected zone HAZ, $t_{8/5}$ cooling time

1. Introduction

The use of high-strength steels (HSS) enables the construction of slender structures with large spans. Due to the high strength of the material cross-sectional dimensions, particularly in the tensile area, can be reduced, leading to lower construction weight. As a result, the material requirement for substructures can also be decreased contributing to a better environmental balance for the entire structure.

Efficient use of high-strength steel may require the use of butt-welded mixed connections of normal and high-strength steel. For example, in lightweight structures, this enables to adjust the strength to the moment distribution instead of varying the plate thickness. Avoiding changes of plate thickness and the normally required mechanical preparation of the plates in the area of butt joints lead to an improved environmental balance, while reduced plate thicknesses and weld seam volumes also allow for cost savings.

Gas metal arc welding (GMAW) is commonly used for welding thin plates of high-strength structural steels due to its high productivity and efficiency. However, GMAW of high-strength structural steels is challenging due to the increased risk of heat-affected zone (HAZ) cracking, distortion, and reduced toughness. Heat management is one of the key challenges in GMAW of thin plates of HSS. For the avoidance of hydrogen cracking in structural steels the carbon equivalent CEV according to Method B in EN 1011-2 [1] (see Table 1) is taken into account. However, this will not be the scope of this research item since preheating is not required for small thicknesses. [2]

One essential measure for the welding of these steels is the cooling time $t_{8/5}$ representing the time needed, during cooling, for the weld run and its HAZ to pass through the temperature range from 800 to 500 °C. Therefore, long $t_{8/5}$ cooling times indicate low cooling rates - temperature over time –, whereas short $t_{8/5}$ cooling times indicate rapid cooling conditions. Within this temperature interval, austenite-ferrite transformation (Ar3 temperature) occurs

https://doi.org/10.1002/cepa.2265 wileyonlinelibrary.com/journal/cepa

causing a change from cubic face-centered to cubic body-centered lattice structure. These materials act brittle and show cold cracking phenomena due the formation of martensite (highly strained body-centered tetragonal form) as a result of short cooling time $t_{8/5}$ in conjunction with a *CET* value (Carbon Equivalent Thyssen) above a certain level according to EN 1011-2 Method B. In addition to this, various researches [3–8] have already shown a softening within the HAZ possibly leading to a failure of these connections contrary to the findings for GTAW welding done by [9]. Some are also using the cooling time $t_{8/5}$ as a measure for the energy input [3; 5; 8; 10] ranging from 5 to 20 s using GMAW. In order to define a suitable welding procedure the cooling time $t_{8/5}$ can be calculated according to EN 1011-2 [1; 11] based on an numerical solution of the 2-dimensional heat transfer using the following equation (1).

$$t_{8/5} = (4300 - 4{,}3 \cdot T_0) \cdot 10^5 \cdot \frac{Q^2}{d^2} \cdot \left[\left(\frac{1}{500 - T_0}\right)^2 - \left(\frac{1}{800 - T_0}\right)^2\right] \cdot F_2 \quad (1)$$

were $$Q = E \cdot k = k \cdot \left(\frac{P_{\text{arc}}}{v_w}\right) \quad (2)$$

and $$P_{\text{arc}} = \frac{1}{T}\int_T [U(t) \cdot I(t)]dt \quad (3)$$

T_0	initial temperature	d	plate thickness
Q	heat input	E	arc energy
F_2	weld shape factor	P_{arc}	electric arc power
k	relative efficiency	U	arc voltage
v_w	welding speed	I	welding current

The predicted cooling times and the measured actual cooling times within this research project [10] are listed in Table 2. In [7] Spiegler developed a design concept based on findings gained for material thicknesses of 10 mm and larger in [8]. Due to the softening in the HAZ losses in the tensile strength of up to 15 % were found. Those findings match with the experimental and theoretical observations from Mauer et al [5]. The developed design concept is given in equation (4).

$$\sigma_{\text{w,Rd}} = \frac{0{,}85 \cdot (0{,}9\, f_{\text{u}}) + 0{,}15\, f_{\text{u,FM}}}{\gamma_{\text{M2}}} \quad (4)$$

with the following factors:

f_{u}	nominal ultimate tensile strength of the parent material
$f_{\text{u,FM}}$	nominal ultimate tensile strength of the filler metal
γ_{M2}	partial factor (1,25 for welds)

The welding-related softening is taken into account by the factor 0,9. The equation applies to full penetration butt welds with steels grades from S460 to S700. It is possible to use filler metals with lower (undermatching), equal (matching) and higher (overmatching) strength compared to the base metal. For steel grade S460, equation (4) can be used for matching and overmatching filler metals. This design concept was accepted by the responsible working group CEN TC250/SC 3/WG 8 and is integrated in FprEN 1993-1-8 [12].

For mixed connections of normal-strength and high-strength steel, according to EN 1993-1-8 [13] and EN 1993-1-12 [14] for full penetration butt welds, the load-carrying capacity is equal to that of the weaker connected component. For normal strength connections according to EN 1993-1-8 [13], the filler metal must meet the minimum strength values of the base material. Therefore, the filler metal must be oriented towards the higher strength connected steel. In the context of [10], extensive experimental investigations are analysed to determine whether this approach is necessary and whether the formation of a soft zone in mixed connections is relevant to the load-carrying capacity of butt joints. This work focuses on the welding of the mixed and matched connections of the plate thickness of d = 3 mm. Within this research project [10] additional 180 experimental tests on butt-welded mixed connection are carried out for plate thicknesses of d = 10 and 20 mm [15].

2. Experimental observations

2.1 Experimental program

In this research, a total of 44 mixed connection and 32 matched connections of 3 mm plates were investigated by measuring the tensile strength, spatially resolved cooling times $t_{8/5}$ and the distortion level and observing the influence of the varying factors:

- base material and filler metal (see Table 1)
- heat input and weld preparation (see Table 2)
- weld upset (see Figure 2)
- backing method (see Figure 2)

The production of the test specimens consists of four basic steps which are described in more detail later.

- Welding of butt joints with IR recording and high frequency real-time data acquisition
- Marking welded plates and 3-D surface scan
- Extracting 4 tensile samples (2 as welded and 2 with removed weld reinforcement)
- Transverse tensile strength tests and ultrasonic contact impedance (UCI) hardness mapping

Table 1 Chemical composition of used materials

Material	C [wt%]	Si [wt%]	Mn [wt%]	P [wt%]	S [wt%]	Cr [wt%]	Ni [wt%]	Mo [wt%]	Cu [wt%]	Al [wt%]	Ti [wt%]	B [wt%]	Nb [wt%]	V [wt%]	N [wt%]	*CEV* [1] in %	*CET* [2] in %
S355J2+N	0,165	0,017	1,560	0,009	0,0030	-	-	-	0,010	0,041	-	-	-	-	0,0047	0,426	0,322
S460MC	0,075	0,015	1,030	0,010	0,0034	0,050	0,010	0,004	0,010	0,050	0,002	0,0002	0,047	0,051	0,0037	0,269	0,182
S700MC	0,062	0,038	1,890	0,007	0,0008	0,035	0,025	0,012	0,013	0,053	0,133	0,0002	0,046	0,007	-	0,390	0,255
G46	0,080	0,960	1,670	0,009	0,009	0,030	0,010	0,01	0,006	0,002	0,011	0,0004	0,001	0,002	0,0020	0,368	0,250
G79	0,100	0,760	1,740	0,010	0,009	0,320	1,820	0,530	0,025	0,005	0,058	0,0010	0,003	0,004	0,0065	0,563	0,394

[1] Carbon equivalent acc. to IIW / EN 1011-2 – Method A: *CE* = *CEV* = C + Mn/6 + (Cr + Mo + V)/5+ (Ni + Cu)/15 in %
[2] Carbon equivalent acc. to EN 1011-2 – Method B: *CET* = C + (Mn + Mo)/10 + (Cr + Cu)/20+ Ni/40 in %

The base materials used was a S355J2+N hot rolled non-alloy structural steel representing the normal strength steel. In addition, a thermomechanical rolled S460MC and S700MC as steel plates of d = 3 mm are used. The filler metal used within these experimental observations were G46 and G79 as Ø1,0 mm solid wire electrodes. The chemical composition of the filler metal and base materials are listed in Table 1.

Table 2 Used materials, weld settings and resulting average and cooling times

Base material	Filler metal	Basic setting	Heat input Q [kJ/mm][1)]	Cooling time $t_{8/5}$ [s]
EN 10025-2-**S355J2+N** (1.0577)	ISO 14341-A **G46** 5 M21 4Si1 (Ø1,0 mm)	Short arc, 5 m/min wire feed rate, V-grove (low heat input)	0,23-0,24	6,5-8,7 [2)] (7,1-7,4)[3)]
EN 10149-2-**S460MC** (1.0982)	ISO 16834-A **G79** 5 M21 Mn4Ni1,5CrMo (Ø1,0 mm)	Pulsed arc, 7,5 m/min wire feed rate, I-Joint (high heat input)	0,44-0,47	9,8-19,3 [2)] (24,4-28,1)[3)]
EN 10149-2 **S700MC** (1.8974)				

[1)] Measured according to equation (2) using k = 0,8
[2)] average measured value for the entire weld seam
[3)] calculated value range using equation (1) inserting T_0 = 20 °C and F_2 = 1

The welds were performed as single layer welds using two procedures with the same welding speed of 45 cm/min, see Table 2. One for high heat input within the applicable range and one representing a low heat input. For low heat input welding a single-V edge preparation with 60° groove angle was chosen, and welding was performed with a wire feed rate of 5 m/min using short arc transfer mode. The high heat input welding was carried out without edge preparation using a wire feed rate of 7,5 m/min with a short free pulsed arc. The used shielding gas for all welding trails complies with ISO 14175 – M21 – ArC – 82/18 [16].

2.2 Welding procedures and verification

The welding samples were clamped onto a welding table using various backing methods, see Figure 1c) to d). The fully mechanized welding was carried out by using a 6-axis Kuka KR60HA robot handling system equipped with a Fronius TPS 500i welding machine. While welding, the process parameters were recorded using a high frequency real time data acquisition system DeweSoft Sirius STG+ with a sampling frequency of 50 kHz. The obtained average heat inputs ranges for the setting using the low and high energy input measured during all trails is listed in Table 2.

The cooling time $t_{8/5}$ was measured using infrared thermographic camera (InfraTec, VarioCAM 3200) recoding the welding process with 100 Hz within the range from 400 to 1200 °C. The emission coefficient ε = 0,8 was verified by thermocouples type C welded into specimens as seen in Figure 1a). The variance for this specimen show a low difference in the determined cooling time $t_{8/5}$ between the thermocouples and IR-camera in the range 0,1 and 0,4 s and nearly identical cooling curves, see Figure 1b).

Instead of only using single spots for the determination of the cooling time $t_{8/5}$, all pixels of the thermographic recoding were analysed to generate a two dimensional pixel map showing an average cooling time of 19,3 s with a fluctuation from 8 to 26 s as shown in Figure 1a) and described in [3]. These tests were carried out using a flat copper bar as backing for the welds with a gap of 0,2 mm between the workpiece and backing bar, see Figure 1c). In addition, an angle copper backing bar, see Figure 1d), was used in direct contact to the welded specimen as well as a ceramic backing, see Figure 1e).

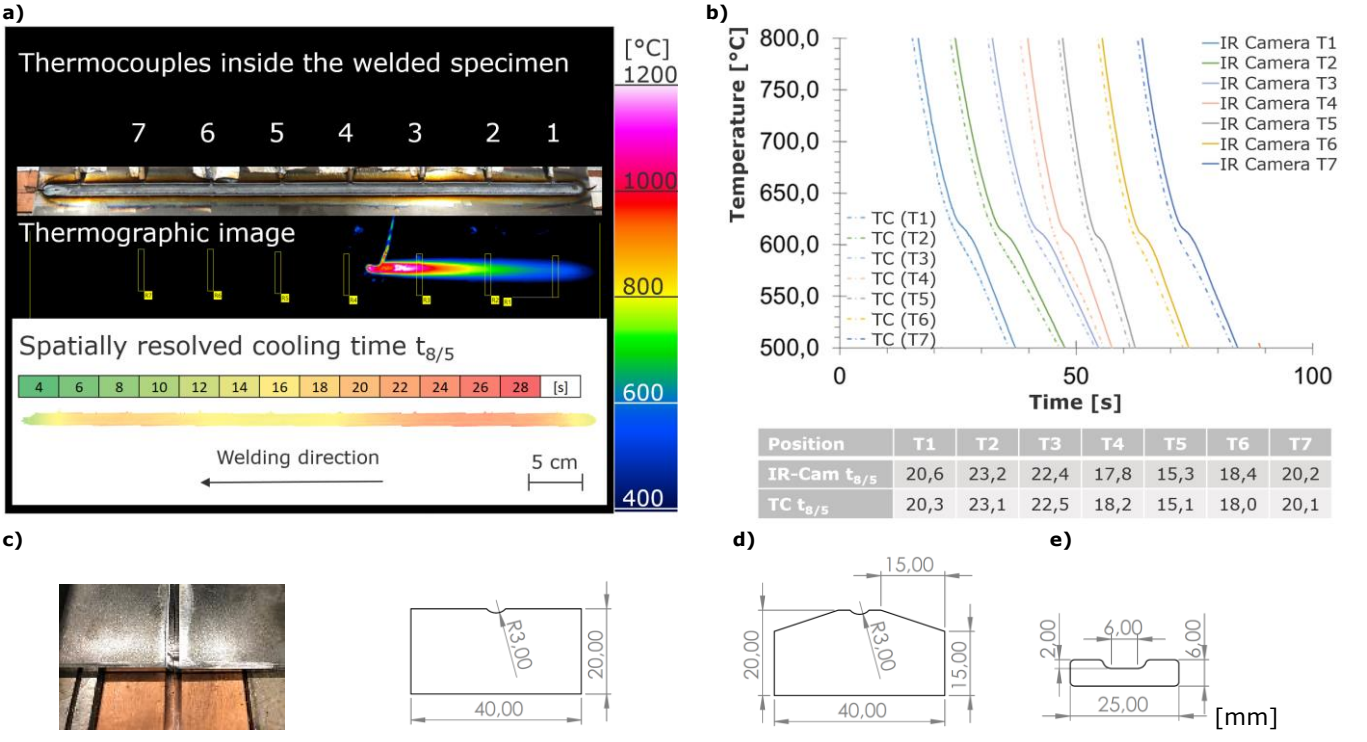

Position	T1	T2	T3	T4	T5	T6	T7
IR-Cam $t_{8/5}$	20,6	23,2	22,4	17,8	15,3	18,4	20,2
TC $t_{8/5}$	20,3	23,1	22,5	18,2	15,1	18,0	20,1

Figure 1 a) Verification measurement using a flat copper bar as backing with spatially resolved cooling time, b) temperature curves for TC-Type C and line measurement using an IR-camera with ε = 0,8, c) flat copper backing bar, d) angle copper backing bar, and e) ceramic backing bar

2.3 Transverse tensile testing

The transverse tensile test were carried out according to ISO 6892-1 [17] at a constant speed of 0,9 mm/min until fracture occurred. A 400 kN Schenck testing machine was used. The setup as well as the geometric dimensions of the specimens are illustrated in Figure 2. The elongation was measured by using the synchronized stereo optical measuring system GOM ARAMIS allowing a locally resolved high resolution measurement of the elongation by analysing a random grayscale pattern, see Figure 2a).

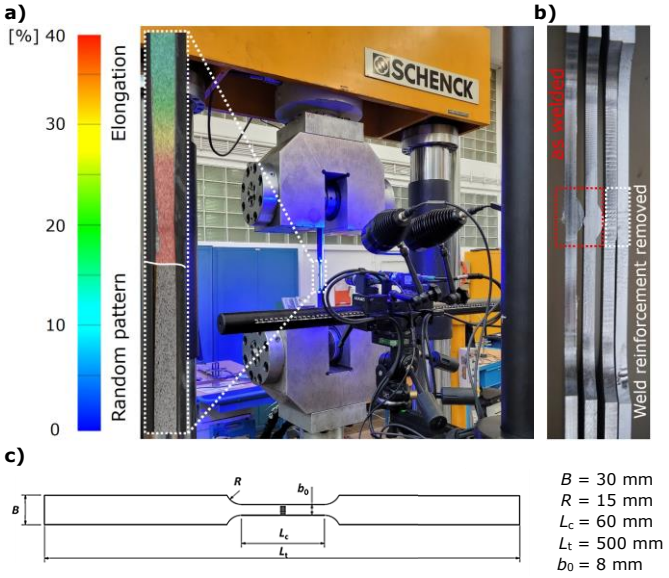

Figure 2 a) Setup for transverse tensile test with ARAMIS measuring system, b) samples with and without weld reinforcement, and c) test sample geometry

Since the hardness correlates directly with the tensile strength and even can be directly converted according to ISO 18265 [18] high resolution hardness mappings were carried out. An automated hardness-testing scanner BAQ UT 200 applying the UCI measuring method with the output scale of Vickers HV 0,1 was used. The scan was made in a square grit with a 0,1 mm stepping width. The validation and calibration of the method were performed by a Struers Durascan optical measuring hardness testing device using also the HV 0,1 scale. Comparative measurements for the calibration and validation gave good results in [3]. The compared areas of 16 mm² showed a variance of the hardness values between the two methods within the standard deviation of these fields.

3. Results and discussion

3.1 Cooling time and micro hardness

For the welding sample depicted in Figure 3a), hardness mappings were created in five sections with different cooling times $t_{8/5}$ (ranging from 6,5 to 14 s). The precise assignment of cooling times is possible based on the surface scans for distortion measurement that were taken before removing the tensile samples. The hardness mappings show a strongly pronounced soft zone in the S700MC. In Figure 3b), the hardness mappings are presented sorted by ascending local cooling time. It becomes clear that with increasing $t_{8/5}$ time, the hardness in the weld metal as well as the hardening in the heat affected zone (HAZ) of the S355J2+N decrease and the size of the soft zone in the S700MC increases. The lowest hardness values of the welded joint occur despite of strongly fluctuating $t_{8/5}$ times in the base material of the normal strength steel S355J2+N.

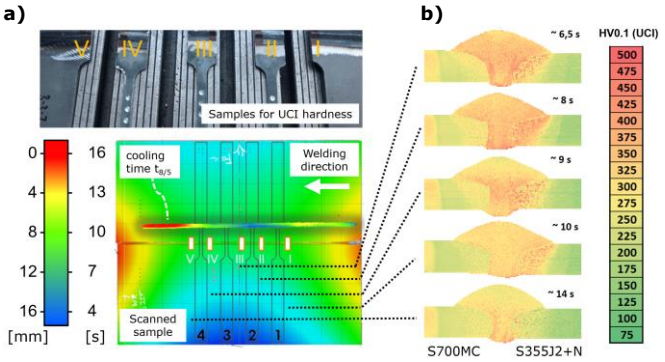

Figure 3 a) Scanned high heat input weld sample overlayed with $t_{8/5}$ cooling time and distortion, b) correlating UCI hardness mappings sorted according to $t_{8/5}$ cooling time

A possible explanation for the fluctuation within the cooling time may be an inconsistent heat convection due to the contact of the weld root with the backing bar. When comparing the locally resolved cooling time of the three backing methods (Figure 4) this becomes obvious, since the fluctuations are found to be much smaller when using an angle copper bar without gap or a ceramic backing. The cooling time by using the flat copper bar was about 19,3 s and thus more than 20 % shorter than the calculated value of 24,6 s according to EN 1101-2. The use of an angle copper bar leads to an average cooling time of 9,8 s which more than 60 % lower than the estimated value.

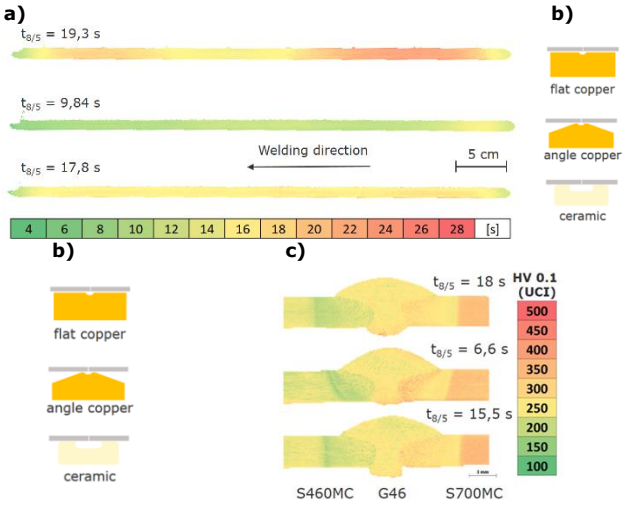

Figure 4 Mixed connection of S460MC on S700MC using G46 with high heat input welding: a) spatially resolved cooling time $t_{8/5}$, b) various backing methods, and c) the resulting UCI hardness

The hardness mapping from Figure 4c) using both copper backing bars are also shown in Figure 5 for the high heat input welding. The area of the soft zone in the HAZ of the S460MC increases from 8,44 to 12,32 mm², and within S700MC from 5,01 to 11,47 mm² for a cooling of $t_{8/5}$ = 6,6 s or 18 s, respectively. The coarse-grained region in the HAZ of the S700MC that resulted for $t_{8/5}$ = 6,6 s seems to soften not as much as for 18 s. Also for the low heat input of 0,23 kJ/mm the coarse-grained seems not to soften for the S700MC while these occurs for the S460MC. The softening compare to the base material

seems higher when using the S700MC, while the reduction of the hardness within the soft zone of the S460MC ranges from 4 to 11 %, the S700MC shows a softening of more than 20 %. This occurs for high as well as low heat inputs.

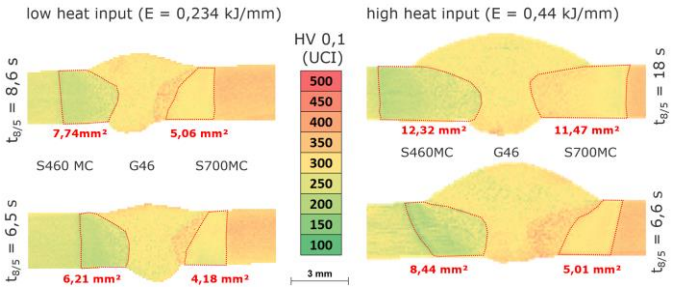

Figure 5 Hardness distribution of mixed connection of S460MC on S700MC with G46 welded with high and low arc energy resulting in different cooling times

3.2 Tensile strength and elongation

The maximum load carrying capacity of the samples σ_{max} was calculated by equation (5) inserting the maximum applied force F_{max} and the initial cross-sectional area S_0 at the location of failure. Therefore, the sample was measured at seven locations prior to the experiment.

$$\sigma_{max} = \frac{F_{max}}{S_0} \tag{5}$$

The results for the maximum load carrying capacities are given in Figure 6, Figure 7 and Figure 8. The results for the welds of S460MC on S460MC shown in Figure 6a. The values of σ_{max} reached are all above characteristic design value for the overmatched filler metal G79 with 591,6 N/mm². Due to the softening in the HAZ the location of failure occurred there - except for two samples tested in as welded condition with low heat input using G46 wire. In these cases the failure was in the base material. The use of an overmatching filler metal did not increase the transversal tensile strength and also the influence of the weld reinforcement removal seems to be neglectable. The values vary in the range of 599,8 to 633,8 N/mm² and also lie all above the tensile strength of the base material.

For the matched connection of S700MC with S700MC (Figure 6b) all samples failed in the HAZ region. Here a significant influence of the filler metal as well as the heat input and the removal of the weld reinforcement is evident. A lower strength filler metal as well as a higher heat input or the removal of the weld reinforcement each lead to a smaller load carrying capacity. The combination of high heat input and the removal of the weld convexity led to σ_{max} = 746,3 N/mm² for one sample, which is slightly below the characteristic design value of 754,3 N/mm². All other samples reached higher values.

All samples of mixed connections S460MC and S700MC (Figure 7) reached load carrying capacities above the tensile strength of the base material S460MC. The influence of the backing method is visualized within the parameter field for the high heat input welding using G46 filler metal. The average load carrying capacity increases by more than 3 % (from 602 N/mm² to 621 N/mm² for the ceramic backing bar and 622 N/mm² for the angle copper bar) when using a different backing bar. The use of a lower heat input resulted in a bigger increase of the load carrying capacity only when using the G46 filler metal. Nevertheless, the G46 seems to be sufficient to achieve a load carrying capacity higher than the tensile strength of the weaker joint partner. Six out of the twenty-four samples cracked in the unaltered base material. An example of the elongation behaviour of these are shown in Figure 9.

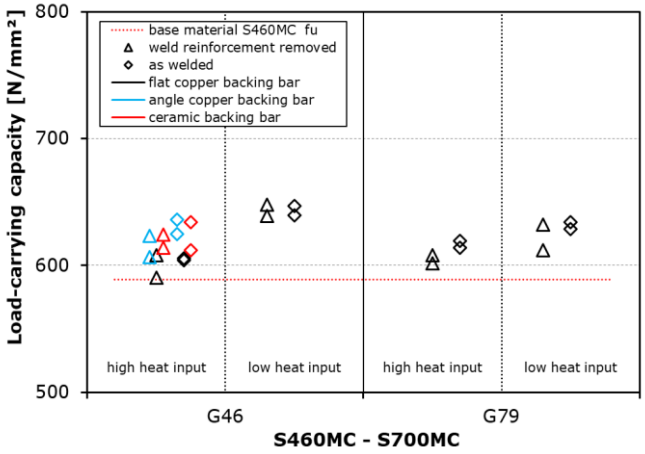

Figure 7 Results for transverse tensile tests of mixed base material S460MC on S700MC welded with G46 and G79

a)

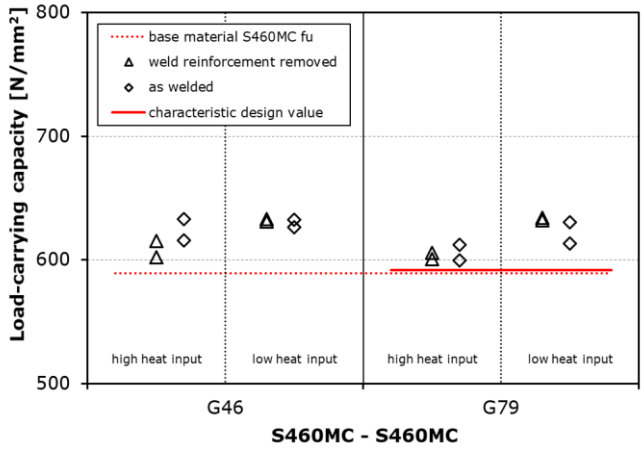

b)

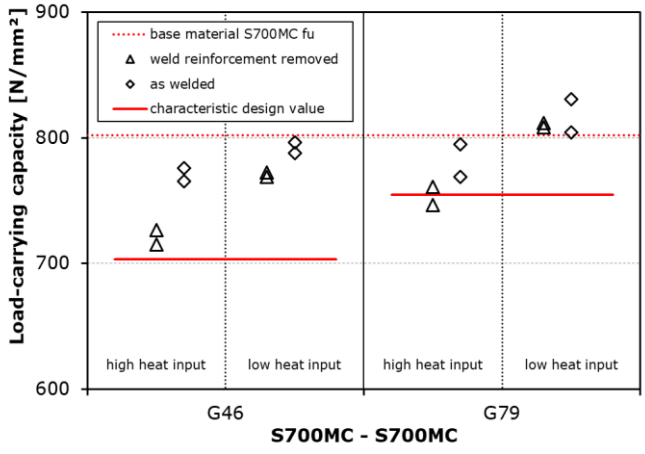

Figure 6 Results for transverse tensile tests of matched base material welded with G46 and G79: a) S460MC on S460MC, b) S700MC on S700MC

All mixed connections of S355J2+N with S700MC (Figure 8) reached the tensile strength of the S355J2+N in the range of 584 ± 10 N/mm². All samples failed in the unaltered S355J2+N base material. No influence of the observed parameter on the tensile strength of the connection was found. Therefore, also the G46 filler metal is sufficient for this type of connection.

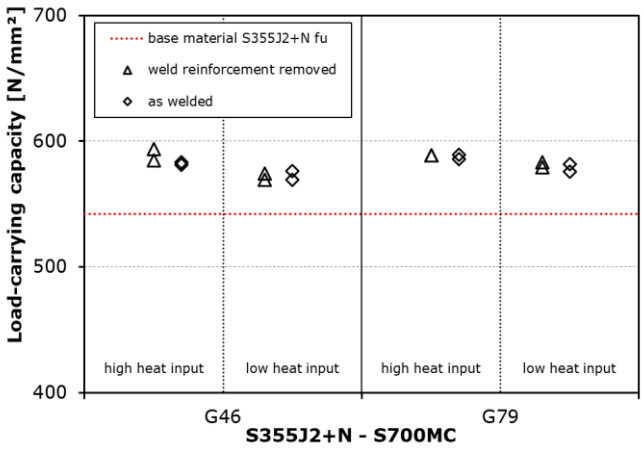

Figure 8 Results for transverse tensile tests of mixed base material S460MC on S700MC welded with G46 and G79

As mentioned, the elongation behaviour in Figure 9 shows a crack of the mixed connection within the base material. During testing, until t = 100 s elongation can only be detected in the HAZ of the weaker joint partner, the S460MC. After 200 s the elongation within the base material increases up to the level of the HAZ after that the elongation within the HAZ "stopped" at approximately 20 % and only the base material keeps stretching until it reaches a local elongation level above 50% leading to a crack. As already shown and discussed in Figure 5 in chapter 3.1, the soften zone of S460MC is only 4% to 11% which is softer than the unaltered base material. Due to the small difference in hardness and the small form of the soft zone in the sample a local increase in strength due to cold work hardening in the soft zone could be a possible explanation for this behaviour.

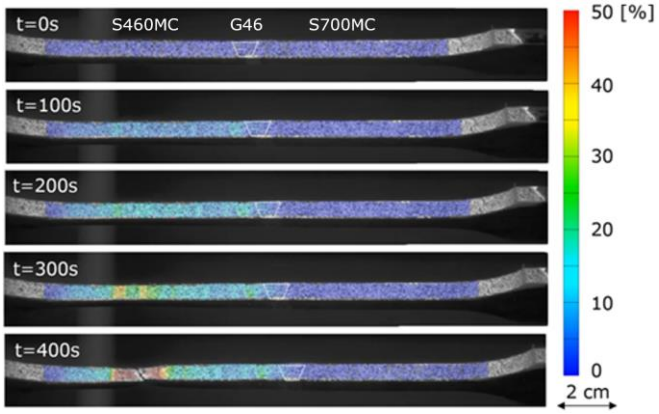

Figure 9 Local elongation of mixed connection sample of S460MC on S700MC using G46 filler with low heat input welding and removed weld reinforcement

3.3 Distortion

In Figure 10 various samples of the 3D-surface scan are shown. After the marking of the samples a GOM ATOS structured light 3D-scanning system was used to scan the welded sample before the extraction of the tensile test specimen. In order to compare the distortion a reference plane was fitted into the scanned sample. The three reference points were located at the two corners at the starting point of the weld and at the end. The two samples on the top and the two samples on the bottom nearly showed the same distortional behaviour. The start and end of the weld were lifted up (positive Z-direction). In addition to this, the determined distortion values in Z-direction were in the same range of -16 to 8 mm although the average $t_{8/5}$ cooling time using the angle copper bar (Figure 10 bottom left) was much lower (9,84 s compare to 19,3 s). The only significant difference can be seen between the samples welded with low heat input. These samples bended toward the other direction.

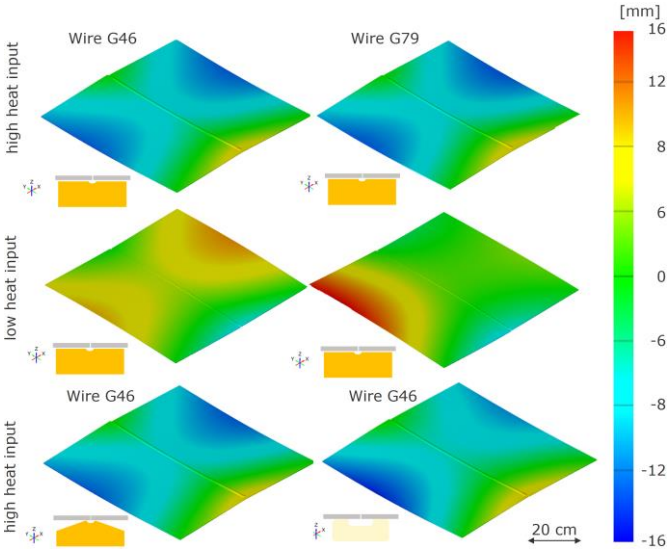

Figure 10 Distortion of welded specimen of mixed connections of S460MC with S700MC for different backing methods, heat inputs as well as welding wires

The reason can be seen in the ratio of weld reinforcement on the top and bottom of the specimen. As seen in Figure 5, the reinforcement area of the weld root was almost the same as the one on the top welding with low heat input. When on the other hand the high heat input leads to a significant bigger reinforcement area on the top compare to the bottom.

4. Conclusion

Within this research project [10] a total of 44 specimen of mixed connection and 32 matched connections of S355J2+N, S460MC and S700MC were welded and analyzed by transverse tensile tests, locally measured cooling times, distortion measurements and hardness mappings HV0,1 (UCI). Based on the results the following conclusions can be drawn:

- For low heat inputs in the range of 0,23 to 0,24 kJ/mm the calculated cooling times $t_{8/5}$ (7,1 to 7,4 s) are within the range of the measured actual ones (6,5 to 8,7 s).
- For high heat input welding (0,44 to 0,47 kJ/mm) the calculated cooling time $t_{8/5}$ (24,4 to 28,1 s) are much longer than the measured actual ones (9,8 to 19,3 s) since the heat dissipation due to backing and/or clamping are not taken into account.
- The highest influence on the local distribution of the cooling time $t_{8/5}$ can be seen for the use of different

backing methods (can more than double) resulting in a significant change of the size of the soft zone.
- The design concept developed by Spiegler in [7] is suitable for plate thicknesses of d = 3 mm for the tested material combinations.
- The results for the mixed connections show an increase of the load carrying capacity for shorter cooling times by using different backing methods.
- For the observed mixed connections with a thickness of d = 3 mm the filler metal matching with the weaker joint partner is sufficient in order to achieve the design load carrying capacity.

5. Acknowledgement

The IGF project "Effective design concepts for welded mixed connections in steel structures" (21412 BG/P 1507) of the Research Association for Steel Application e. V. (FOSTA), Sohnstraße 65, 40237 Düsseldorf, Germany, is a part of the FOSTA joint research program HOCHFEST and was funded by the Federal Ministry for Economic Affairs and Climate Action via the AiF within the framework of the program for the promotion of joint industrial research and development (IGF) on the basis of a resolution of the German Bundestag. Special thanks go to the industrial partners of the project committee for their support of the research project.

6. References

[1] *DIN EN 1011-2:2001-05 (2001) Welding – Recommendations for welding of metallic materials – Part 2: Arc welding of ferritic steels. German version EN 1011-2:2001.*

[2] Xu, K. (2012) *Hydrogen embrittlement of carbon steels and their welds* in: *Gaseous Hydrogen Embrittlement of Materials in Energy Technologies*. Elsevier, pp. 526–561.

[3] von Arnim, M.; Eichler, S.; Brätz, O.; Hildebrand, J.; Gericke, A.; Kuhlmann, U.; Bergmann, J. P.; Flügge, W. (2022) *Effiziente Nachweiskonzepte für geschweißte Mischverbindungen im Stahlbau* in: Stahlbau 91, H. 10, pp. 660–670.

[4] Rahman, M.; Maurer, W.; Ernst, W.; Rauch, R.; Enzinger, N. (2014) *Calculation of hardness distribution in the HAZ of micro-alloyed steel* in: Welding in the World 58, H. 6, pp. 763–770. https://doi.org/10.1007/s40194-014-0156-5

[5] Maurer, W.; Ernst, W.; Rauch, R.; Vallant, R.; Enzinger, N. (2015) *Evaluation of the factors influencing the strength of HSLA steel weld joint with softened HAZ* in: Welding in the World 59, H. 6, pp. 809–822. https://doi.org/10.1007/s40194-015-0262-z

[6] Ran, M.-M.; Sun, F.-F.; Li, G.-Q.; Kanvinde, A.; Wang, Y.-B.; Xiao, R. Y. (2019) *Experimental study on the behavior of mismatched butt welded joints of high strength steel* in: Journal of Constructional Steel Research 153, pp. 196–208. https://doi.org/10.1016/j.jcsr.2018.10.003

[7] Spiegler, J. (2022) *Tragfähigkeit von Kehlnaht- und Stumpfnahtverbindungen höherfester Baustähle – Dissertation. Mittelung Institut für Konstruktion und Entwurf No. 2022-2, University of Stuttgart. http://dx.doi.org/10.18419/opus-12207*.

[8] Bergmann, J. P.; Hildebrand, J.; Kuhlmann, U.; Spiegler, J.; Keitel, S.; Mückenheim, U. (2020) *Tragfähigkeit von Stumpfnähten höherfester Stähle im Stahlbau. (engl.: Load carrying capacity of butt welds made of high-strength steel.) Research report, AiF; IGF-Nr. 19.470 BG; DVS-Nr. 09.083. ISBN: 978-3-96870-458-6*.

[9] Kornokar, K.; Nematzadeh, F.; Mostaan, H.; Sadeghian, A.; Moradi, M.; Waugh, D. G.; Bodaghi, M. (2022) *Influence of Heat Input on Microstructure and Mechanical Properties of Gas Tungsten Arc Welded HSLA S500MC Steel Joints* in: Metals 12, H. 4, pp. 565. https://doi.org/10.3390/met12040565

[10] Kuhlmann, U.; Bergmann, J. P.; Hildebrand, J.; Gericke, A.; Arnim, M. von; Eichler, S.; ongoing Project *Effiziente Nachweiskonzepte für Mischverbindungen im Stahlbau. (engl. Effective design concepts for mixed connections in steel structures.) German Federation of Industrial Research (AiF); IGF-Nr. 21412 BG; FOSTA-Nr. P 1507.*

[11] *DVS-Merkblatt 0916 (2012) Metall-Schutzgasschweißen von Feinkornbaustählen. Technical bulletin. Düsseldorf: DVS Media GmbH*.

[12] *FprEN 1993-1-8:2023 (2023) Eurocode 3 – Design of steel structures – Part 1-8: Design of joints. Formal vote draft.*

[13] *EN 1993-1-8: 2005 + AC:2009 Eurocode 3: Design of steel structures - Part 1-8: Design of joints.*

[14] *EN 1993-1-12: 2007 + AC:2009 Eurocode 3: Design of steel structures - Part 1-12: Additional rules for the extension of EN 1993 up to steel grades S700*.

[15] von Arnim, M.; Eichler, S.; Brätz, O.; Hildebrand, J.; Kuhlmann, U.; Bergmann, J. P.; Flügge, W. (2023) *Study on load carrying capacity of MAG butt-welded mixed connections with different steel strengths* in: EUROSTEEL, Amsterdam.

[16] *EN ISO 14175:2008, Welding consumables - Gases and gas mixtures for fusion welding and allied processes.* Berlin: Beuth Verlag GmbH.

[17] *EN ISO 6892-1:2019 Metallic materials – Tensile testing – Part 1: Method of test at room temperature.*

[18] *EN ISO 18265:2013 Metallic materials – Conversion of hardness values.*